Fullerene nano/microcrystals of unique shapes and controlled size

ARTICLE · NOVEMBER 2009

DOI: 10.1016/j.carbon.2009.07.005

5 AUTHORS, INCLUDING:

Akito Masuhara

Yamagata University

67 PUBLICATIONS **558** CITATIONS

SEE PROFILE

Zhenquan Tan

Dalian University of Technology

45 PUBLICATIONS **263** CITATIONS

SEE PROFILE

Hitoshi Kasai

Tohoku University

213 PUBLICATIONS **3,112** CITATIONS

SEE PROFILE

CARBON 64 (2013) 370–376

Available at www.sciencedirect.com

ScienceDirect

journal homepage: www.elsevier.com/locate/carbon

Thermal-induced shape transformation of solvated C_{60} microcrystals

Zhenquan Tan [a,*], *Akito Masuhara* [b], *Hitoshi Kasai* [c], *Hachiro Nakanishi* [c], *Hidetoshi Oikawa* [c]

[a] *Joining and Welding Research Institute, Osaka University, 11-1 Mihogaoka, Ibaraki, Osaka, Japan*
[b] *Graduate School of Science and Engineering, Yamagata University, Jonan 4-3-16, Yonezawa, Yamagata, Japan*
[c] *Institute of Multidisciplinary Research for Advanced Materials, Tohoku University, Katahira 2-1-1, Aoba-ku, Sendai, Japan*

ARTICLE INFO

Article history:
Received 21 March 2013
Accepted 5 July 2013
Available online 31 July 2013

ABSTRACT

Phase transformation of solvated C_{60} microcrystals (MCs) was directly observed for the first time by use of thermal treatment to induce the phase transformation. C_{60} MCs were changed from bundle rod-shape to disc-shape, accompanied with the change of crystal structure from $P6_3$ symmetry to *fcc* symmetry. This kind of phase transformation included three steps in solvent medium: exchange of incorporated solvent, decomposition of old crystals, and formation of new crystals. It is not likely a kind of crystal-to-crystal phase transition assisted by incorporation of dispersing solvents but can be demonstrated as a decomposition–recrystallization process. The mechanism has been also tested by the thermal-induced phase transformation of C_{60} MCs from bundle shape to bipyramid shape.

1. Introduction

Recently synthesis of shape-tailored low-dimensional fullerene C_{60} microcrystals (MCs) has attracted tremendous attention [1–13], and promises a wide range of applications from high temperature superconductors [14,15] and solar cells [16,17] to organic field-effect transistors [18]. Many approaches have been reported for the formation of low-dimensional fullerene C_{60} MCs. For example, liquid–liquid interfacial precipitation (LLIP) is a widely used solution approach to synthesize one-dimensional C_{60} nanowiskers [1,3]. On the other hand, a solution route of self-assembly was generally used to synthesize low-dimensional nanostructures of C_{60} derivatives by utilizing the molecular interactions between C_{60} and the terminal groups [9–12]. In previous research, we have reported that the reprecipitation method, which was a general solution approach to synthesize organic nanocrystals [19,20], was very efficient in the synthesis of shape-tailored low-dimensional C_{60} MCs [6,7,21]. The shape, the crystal structure, and the size distribution of C_{60} MCs were strongly dependent on the reprecipitation parameters such as solvent species, temperature, and volume ratio of good to poor solvent. Solution-grown C_{60} MCs are almost solvated crystals, in which the incorporated solvent molecules act as a controller for tuning the shape of C_{60} MCs [5–7,22]. If removing the incorporated solvent molecule from C_{60} MCs in vacuum or in atmosphere, C_{60} MCs showed crystal-to-crystal phase transition behavior that the crystal structure changed correspondingly with the removing internal incorporated solvent but the shape does not changed during the phase transition [2,23–26]. Sathish et al. reported that the shape of two-dimensional C_{60} nanosheets shifted to one-dimensional nanorods by water treatment and suggested a solvent engineering approach for shape-control of C_{60} MCs [27]. Recently we found that if tuning a solvated C_{60} MCs in another selected solvent medium, they showed a novel phase transformation behavior that both the shape and the crystal structure changed with the exchange of internal incorporated solvent induced by ultrasonication

* *Corresponding author:* Fax: +81 668794370.
E-mail address: zq-tan@jwri.osaka-u.ac.jp (Z. Tan).
0008-6223/$ - see front matter
http://dx.doi.org/10.1016/j.carbon.2013.07.087

treatment [28]. By carefully selecting the solvent mediums, a cyclic transformation was also achieved that had a cyclic route of rod-disc-belt-rod. This novel behavior has been of many research interests ranged from fundamental researches of solid state to synthesis of shape-tailored low-dimensional nanomaterials. However, ultrasonication generates high energy in a micro-space [29,30] and quickly damages C_{60} MCs, which has limited the observation of the shape change during the phase transformation.

Here we report an observation of the thermal-induced phase transformation of solvated C_{60} MCs by exchanging the incorporated solvent internal C_{60} MCs in a selected solvent medium. Thermal treatment provides a mild surrounding for slow phase transformation, which enables us to directly observe the details of the phase transformation. We found that the phase transformation assisted by exchange of incorporation solvents was not likely a kind of crystal-to-crystal phase transition but could be demonstrated as a decomposition-recrystallization process. Our study is helpful to improve the understanding on the crystallization and phase transformation of solvated crystals.

2. Experimental

C_{60} powder (>99.5%) was purchased from Tokyo Kasei Industry Co., Ltd. (Tokyo, Japan) and used as received. *m*-xylene (⩾99%), ethanol (⩾99.8%), and 2-propanol (⩾99.5%) were commercially available, and all used without any further purification. Approach for formation of C_{60} MCs and their thermal-induced phase transformation has been shown in scheme 1. Firstly, C_{60} MCs that used as a starting material were fabricated by the reprecipitation method [19,20]. A 50 μl of *m*-xylene solution of C_{60} (2 mM) was quickly injected into 10 ml of vigorously stirred 2-propanol. The dispersion liquid was allowed to age for 4 h for the growth of C_{60} MCs. Afterwards, as-grown C_{60} MCs were filtrated onto a polymeric membrane filter. The thin film of C_{60} MCs on membrane filter was immersed into ethanol in a constant 40 °C water bath. Because the phase transformation performed in a mild thermal condition and used C_{60} film supported by filter which can be investigated directly, it was possible to observe the details of the phase transformation in comparison with ultrasonication-induced phase transformation. The time-resolved changes on shape and crystal structure were investigated by scanning electron microscopy (SEM, JEOL JSM-6700F, Japan) and powder X-ray diffraction (XRD, Bruker AXS M18XHF22, Germany), respectively. A mass spectroscopy was carried out for the detection of C_{60} molecules in the ethanol solution during the phase transformation process (JEOL AccuTOF-DART, Japan).

3. Results and discussion

C_{60} MCs were loaded on membrane filter that could be directly used to SEM investigation, which allowed us to observe the morphology change via in situ testing. Fig. 1 shows time-resolved SEM images of C_{60} MCs after thermal treatment in ethanol. Fig. 1a shows as-grown C_{60} MCs fabricated by the reprecipitation method. The as-grown C_{60} MCs have a hexagonal bundle-rod shape and a monodispersed size distribution. This kind of C_{60} MCs was single crystal achieved mainly influencing by the concentration depletion of C_{60} molecules at the end-edge of the growing face [5,7,31], but not self-assembly of one-dimensional nanorods reported by Qu et al. [32]. The bundle-shaped C_{60} MCs was considered having low thermodynamic stability and easily happened phase transformation because of the large surface area and more surficial defects. After 5-min thermal treatment, some C_{60} MCs had begun to change from bundle shape to disc shape (Fig. 1b). The disc-shaped C_{60} MCs were also a hexagonal shape. In previous research, we have found that as-grown bundle-shaped C_{60} MCs were solvated crystal containing

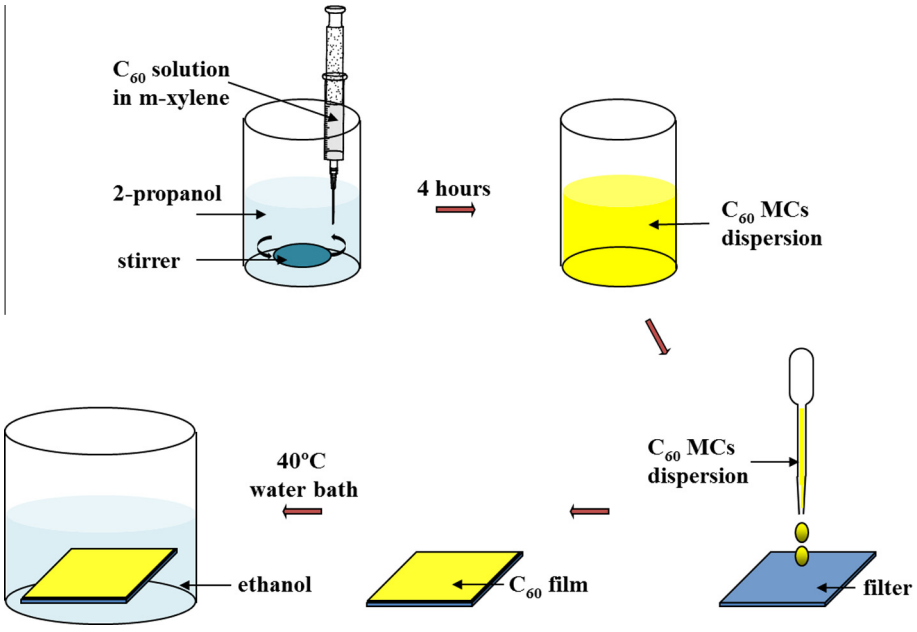

Scheme 1 – Schematic illustration for the thermal-induced phase transformation of C_{60} MCs.

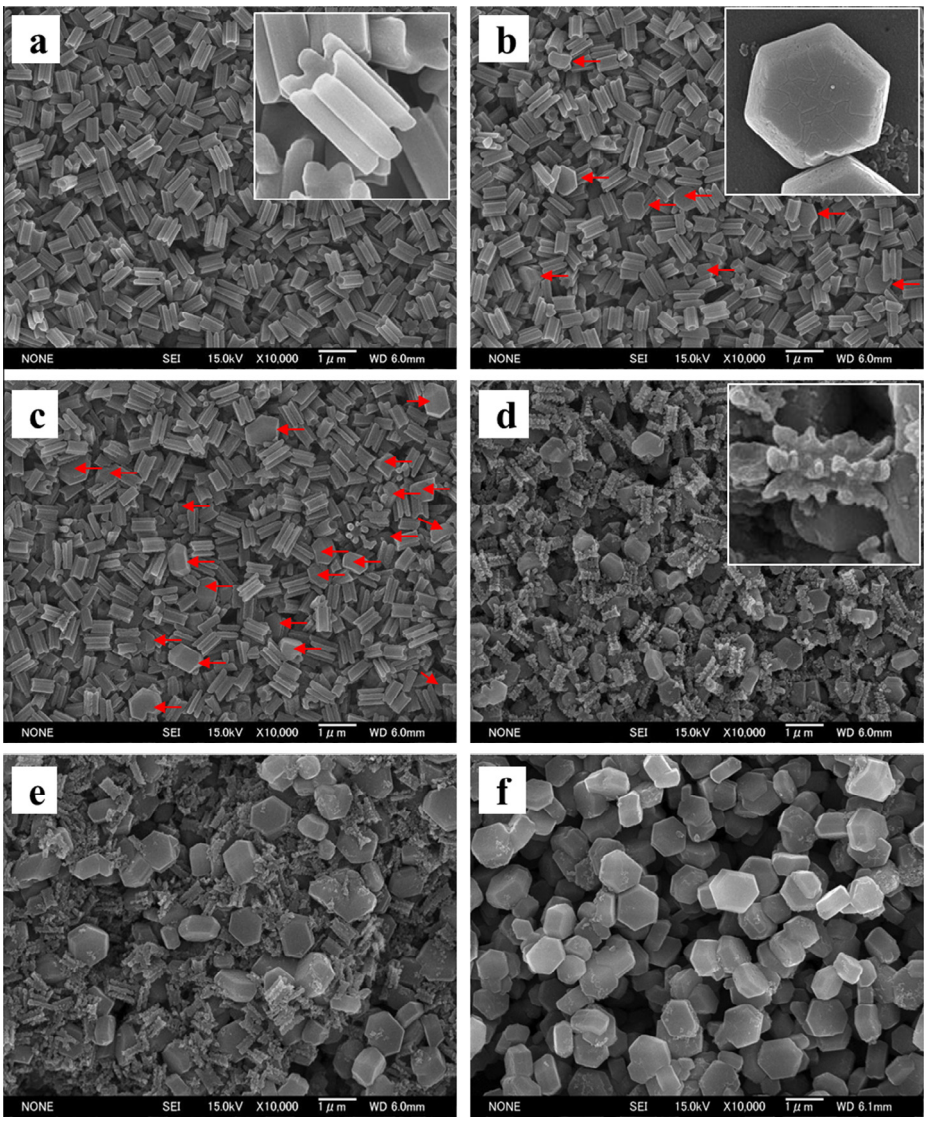

Fig. 1 – SEM images of thermal-induced phase transformation from C60 bundle rod shape to disc shape after heated at 40 °C for (a) 0 min, (b) 5 min, (c) 10 min, (d) 20 min, (e) 30 min, and (f) 60 min. Insets in (a), (b), (d) show as-grown bundle-shaped, disc-shaped, and semi-decomposed C60 MCs. The red arrows indicate the disc-shaped C60 MCs. (For interpretation of the references to colour in this figure legend, the reader is referred to the web version of this article.)

~10% of *m*-xylene as well as the disc-shaped C_{60} MCs were solvated crystal containing ~3% of ethanol [6,7]. The phase transformation was thus speculated mainly due to the exchange of incorporated solvent ligands from *m*-xylene to ethanol internal crystal in which the incorporated solvent acted as a shape controller [28]. As shown in Fig. 1c–f, the statistical number of disc-shaped C_{60} MCs increased with heating time. Especially, after thermal treated for more than 20 min, a great deal of C_{60} MCs changed from bundle to disc shape. A high magnification SEM image of bundle-shaped C_{60} MCs shows that the C_{60} MCs were almost semi-decomposed. C_{60} molecules on the crystal surface were broken away from the crystal during the solvent ligands exchange. The separated C_{60} molecules were re-solvated by surrounding ethanol molecules and contributed to the formation of new phase of C_{60} crystals. After 30 min, most of bundle-shaped C_{60} MCs were decomposed to many small pieces (Fig. 1e). The thermal-induced phase transformation of C_{60} MCs was completed within 60 min at 40 °C that all C_{60} MCs changed from bundle-shape to disc-shape (Fig. 1f).

The crystal structure of C_{60} MCs also changed with the exchange of incorporated solvent ligands during the phase transformation. As-grown bundle-shaped C_{60} MCs have a $P6_3$ crystal structure and are solvated crystals containing *m*-xylene molecules (Supporting information, Part 1), which was the same to other rod-shaped C_{60} MCs that grown from the *m*-xylene (good solvent)/2-propanol (poor solvent) system [6]. We have also found that the disc-shaped C_{60} MCs is face-centred cubic (*fcc*) lattice with a cell parameter of $a = 14.19$ Å (Supporting information, Part 2). Time-resolved change on crystal structure from $P6_3$ to *fcc* was investigated by XRD measurement during the phase transformation of C_{60} MCs from bundle-shape to disc-shape (Fig. 2). After 5-min thermal treatment, the crystal structure was still mainly $P6_3$. However, a

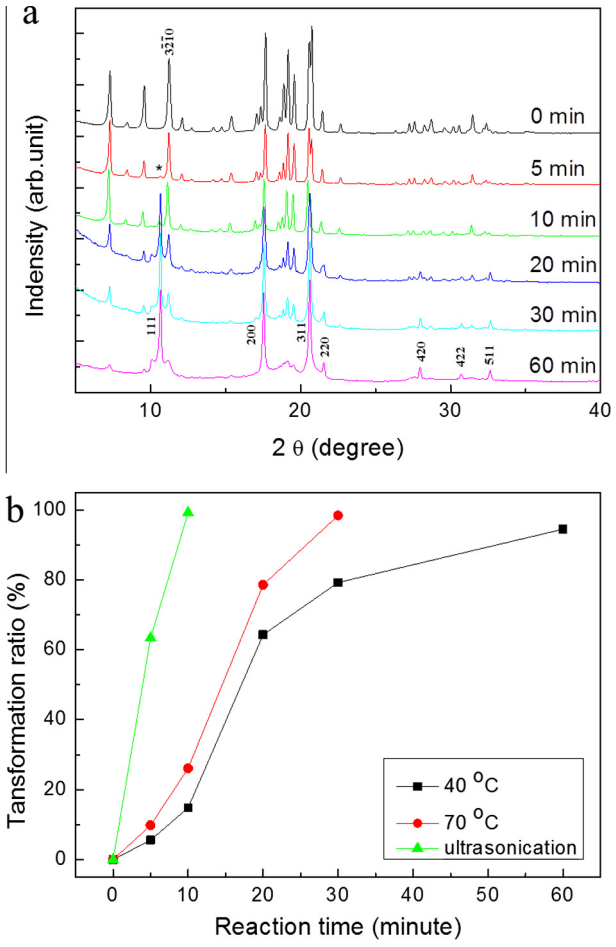

Fig. 2 – Time-resolved powder XRD patterns (a) and transformation ratio (b) of C60 MCs in thermal-induced phase transformation. * Mark indicates the (111) diffraction of *fcc* crystal structure. Thermal-induced phase transformation at 70 °C and ultrasonication-induced phase transformation were performed as references in (b).

small new peak appeared at $2\theta = 10.6°$, which was assigned to (111) diffraction of *fcc* lattice. The appearance of (111) diffraction indicated the formation of disc-shaped C_{60} MCs, which is in agreement to the SEM observation shown in Fig. 1b. The (111) diffraction from *fcc* structure increased with heating time accompanied with the reduction of diffraction peaks from $P6_3$ structures. At the case of 20-min thermal treatment, the intensity of (111) peak from *fcc* structure dominated the neighboring (3 −2 −10) peak from $P6_3$ structure at $2\theta = 11.2°$. The formation of a great deal of disc-shaped C_{60} MCs had been already conformed by SEM observation (Fig. 1d). After 60 min treatment, the diffraction peaks were mainly assigned to (111), (200), (311), (222), (420), (422), and (511) according to *fcc* crystal structure, which indicated that bundle-shaped C_{60} MCs having $P6_3$ structure mostly transformed to disc-shaped C_{60} MCs having *fcc* structure.

The transformation ratio from $P6_3$ to *fcc* was defined as $\emptyset = I_{fcc}/(I_{fcc} + I_{p63})$, where *I* was the intensity of diffraction peak. (3 −2 −10) peak from $P6_3$ structure and (111) peak from *fcc* structure were selected to evaluate the transformation ratio. Fig. 2b shows the calculation result. The transformation rate *c* was defined as $c = d\emptyset/dt$. We found that the transformation rate at 40 °C gradually increased and reached maximum at around 15 min, and then gradually slowed down with the decomposition of $P6_3$ C_{60} MCs (Fig. 2b). We have also observed the crystal structure change at 70 °C to investigate the temperature effect in the thermal-induced phase transformation. The phase transformation of C_{60} MCs at high temperature was faster than that at low temperature. In roughly 30 min all C_{60} MCs changed from $P6_3$ to *fcc*. As a reference, ultrasonication treatment was also performed to induce phase transformation by use of the bundle-shaped C_{60} MCs as starting material. The ultrasonication-induced phase transformation was finished within 10 min, which mainly due to the strong collapsing force generated by ultrasonication for decomposition of C_{60} MCs [29,30]. On the other hand, in comparison of ultrasonication-induced phase transformation using C_{60} MCs having bundle shape in this study and rod shape in previous study [28], the bundle-shaped C_{60} MCs are much easily damaged and transformed to other phase, which allows the bundle-shaped C_{60} MCs a suitable material for the mechanism research of the thermal-induced phase transformation in solvent medium.

Compare to ultrasonication irradiation, thermal treatment was considered a much milder process that allows us to observe more details of phase transformation and further discuss the microscopic mechanism. Fig. 3 shows high-resolution SEM images of C_{60} MCs at different stage of the phase transformation. Before the phase transformation, bundle-shaped C_{60} MCs had a beautiful morphology. The surface of crystal was very smooth and perfect. When thermal treatment in ethanol, the surface of all bundle-shaped C_{60} MCs became rough (Fig. 3b), which indicated that C_{60} molecules on the surface were decomposed from the crystal accompanied with the ligand exchange that incorporated m-xylene in $P6_3$ structure was exchanged by ethanol molecules. However, the solubility of C_{60} in ethanol was very poor so that ethanol-solvated C_{60} molecules nucleated and grew to a new phase of C_{60} MCs in order to optimize the energy. We found that a new crystal nucleus always connected to an old crystal which has been badly damaged. We supposed that C_{60} MCs having more defects were much easier to be damaged or decomposed than those having less defects. The concentration of decomposed C_{60} molecules thus was high at around those badly damaged crystals, where was easy to form the new nuclear. The growth of a new phase crystal accompanied with the decomposition of old crystal during the phase transformation (Fig. 3c). Our result showed that all old crystals were decomposed and contributed to the formation of new crystals at the same time during the phase transformation, which suggested that it was not a kind of crystal-to-crystal phase transformation that happened by heating in vacuum or in atmosphere [2,23,24], but was a kind of phase transformation that underwent decomposition-recrystallization process assisted by the exchange of incorporated solvent in a selected solvent medium. At the end of the phase transformation (Fig. 3d), a new kind of solvated C_{60} MCs having new crystal structure and new shape was formed, corresponding to the given solvent medium.

Based on the experimental observation, we suggest a general mechanism for the thermal-induced shape transformation of C_{60} MCs. As shown in Fig. 4, two rod-like rectangular

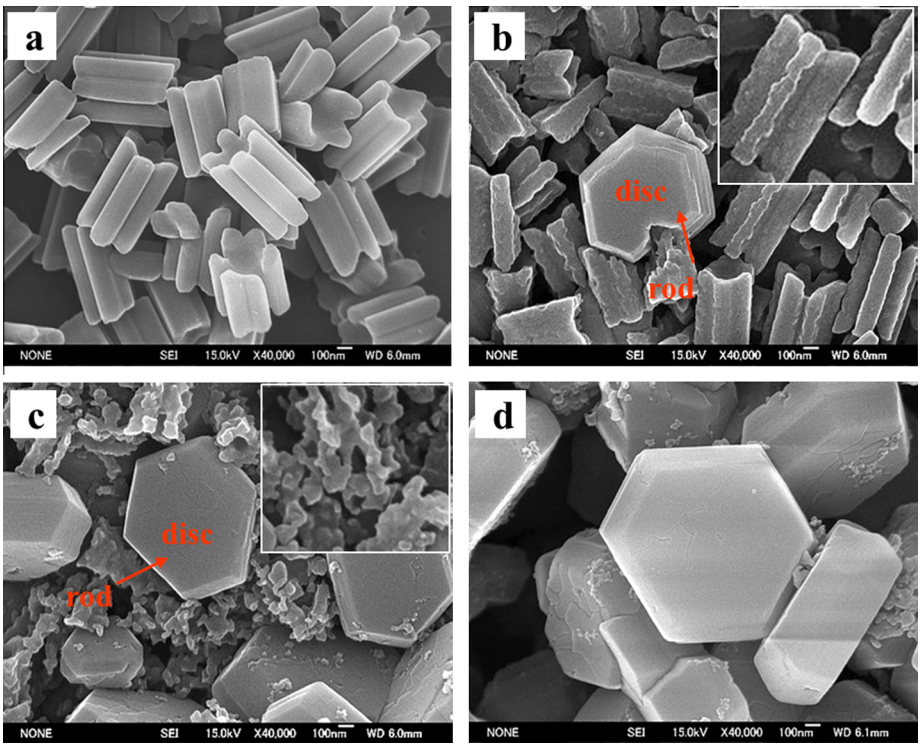

Fig. 3 – High-resolution SEM images of phase transformation from C60 bundle shape to disc shape at different stage of (a) before, (b) at the beginning, (c) at the late period, and (d) at the end of transformation.

grids presented the bundle-shaped C_{60} MCs used in this study. The grid on the left represented C_{60} MCs having many defects. After thermal treatment in ethanol, both C_{60} MCs began to decompose as a result of solvated C_{60} molecules on the surface exchanged the incorporated solvent ligands. In such case, C_{60} MC having many defects was superior to serve as an active site for nucleation of new crystal. The new nucleus grew with the heating time, since the exhausted C_{60} molecules were continuously supplied by the decomposition of old C_{60} MCs. Finally, the decomposition of old phase of C_{60} MCs completely underwent accompanied with the formation of a new phase of C_{60} MCs. This mechanism mainly composed of the decomposition of old phase and recrystallization of new phase, which also had been observed in the ultrasonication-induced phase transformation of C_{60} MCs [28]. Considering that ultrasonication treatment mainly accelerates the phase transformation but not affects the transformation process, the decomposition-recrystallization mechanism is speculated as a general rule for the phase transformation of solvated C_{60} MCs in solvent medium.

According to this decomposition-recrystallization mechanism, an intermediate procedure that C_{60} molecules dissociated into medium assisted by solvent molecules was a key step, which was the main difference to the previous

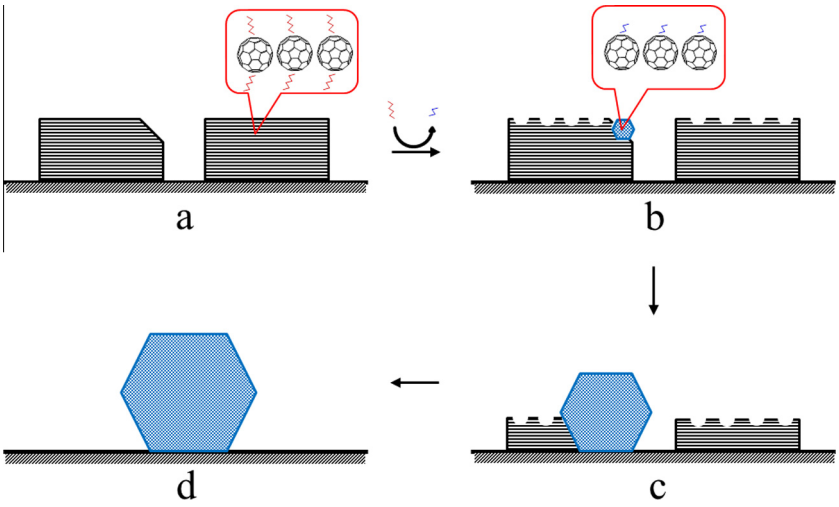

Fig. 4 – Mechanism of thermal-induced phase transformation of C60 MCs from bundle shape to disc shape.

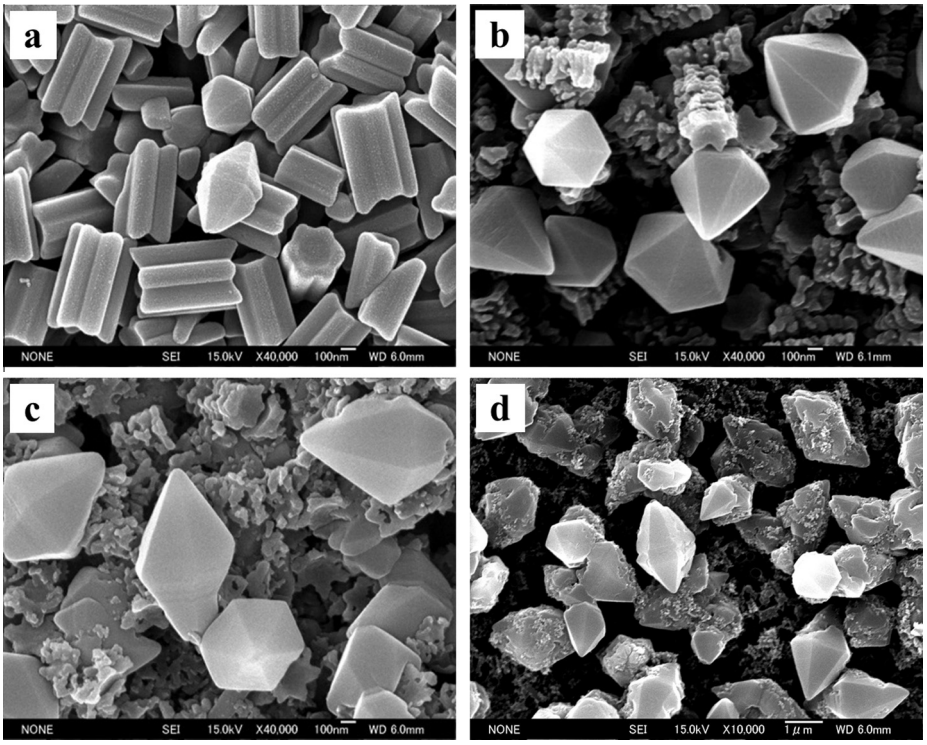

Fig. 5 – SEM images of thermal-induced phase transformation from C60 bundle rod shape to bipyramid shape after heated at 40 °C for (a) 10 min, (b) 30 min, (c) 60 min, and (d) 120 min.

mechanism of crystal-to-crystal phase transition. We measured the mass spectroscopy of the solvent during C_{60} MCs phase transformation from bundle rod shape to disc shape after heated at 40 °C for 30 min. A peak was detected in the solvent at $m/z = 720.89$, which was assigned to ionized C_{60} molecules (Supporting information, Part 4). The mass spectroscopy gave clear evidence that C_{60} molecule dissociated into solvent medium during the phase transformation, which was in good agreement to the decomposition-recrystallization mechanism.

In order to verify the mechanism, another thermal-induced phase transformation was performed. The bundle-shaped C_{60} MCs thin film on membrane filter was immersed into a CS2/ethanol (1:10) mixed solution at 40 °C for thermal-induced phase transformation. Fig. 5 shows that the bundle-shaped C_{60} MCs changed slowly to bipyramid shape having hcp crystal structure (Supporting information, Part 3). This transformation process was well agreed to the decomposition-recrystallization mechanism. On the other hand, if the phase transformation was induced by ultrasonication, the resulting C_{60} was not bipyramid shape but belt shape with a faster transformation rate. Both bipyramid shape and belt shape of C_{60} MCs were also directly prepared by the reprecipitation method in CS2 (good solvent)/ethanol (poor solvent) system with small (for bipyramid) or large (for belt) injecting amount [7,33], which suggested that the concentration depletion at the growing zone determined the shape of bipyramid or belt. In the phase transformation of C_{60} MCs, thermal treatment contributed to a milder surrounding and slower decomposition rate than ultrasonication. Therefore, the low concentration depletion of C_{60} molecules in the thermal-induced phase transformation resulted in the bipyramid-shaped C_{60} MCs. The results of phase transformation were also agreed to the nanocrystals growth in the reprecipitation.

4. Conclusions

A thermal-induced phase transformation of solvated C_{60} MCs has been demonstrated from an as-grown bundle shape to a disc shape. By utilizing the mild thermal treatment, the details of the phase transformation in the solvent medium is observed for the first time. A mechanism is suggested as a general rule for the phase transformation of solvated C_{60} MCs assisted by exchange of incorporated solvents, which can be demonstrated as a decomposition–recrystallization process. C_{60} MCs prepared from solution approaches are always crystal solvates. The incorporated solvent molecules act as ligands to C_{60} and affect the crystal structure and the shape of solvated C_{60} MCs. The phase transformation of C_{60} MCs is a common phenomenon when the incorporated solvent exchanges to another solvent internal the solvated C_{60} MCs [33]. Therefore, C_{60} is a perfect quantum dot with a regular spherical shape and it is a suitable model material to study the crystallization and phase transformation of other organic and inorganic materials. Our study is not only helpful for understanding the mechanism of crystallization and phase transformation of solvated crystals, but also suggests a novel approach to synthesize shape-tailored low-dimensional nanomaterials.

Appendix A. Supplementary data

Supplementary data associated with this article can be found, in the online version, at http://dx.doi.org/10.1016/j.carbon.2013.07.087.

REFERENCES

[1] Minato J, Miyazawa K. Solvated structure of C_{60} nanowhiskers. Carbon 2005;43:2837–41.
[2] Wang L, Liu BB, Liu DD, Yao MG, Hou YY, Yu SD, et al. Synthesis of thin, rectangular C_{60} nanorods using m-xylene as a shape controller. Adv Mater 2006;18:1883–8.
[3] Sathish M, Miyazawa K, Sasaki T. Nanoporous fullerene nanowhiskers. Chem Mater 2007;19:2398–400.
[4] Jin YZ, Curry RJ, Sloan J, Hatton RA, Chong LC, Blanchard N, et al. Structural and optoelectronic properties of C_{60} rods obtained via a rapid synthesis route. J Mater Chem 2006;16:3715–20.
[5] Ji HX, Hu JS, Tang QX, Song WG, Wang CR, Hu WP, et al. Controllable preparation of submicrometer single-crystal C_{60} rods and tubes trough concentration depletion at the surfaces of seeds. J Phys Chem C 2007;111:10498–502.
[6] Tan Z, Masuhara A, Kasai H, Nakanishi H, Oikawa H. Multi-branched C_{60} micro/nanocrystals fabricated by the reprecipitation method. Jpn J Appl Phys 2008;47:1426–8.
[7] Masuhara A, Tan Z, Kasai H, Nakanishi H, Oikawa H. Fullerene fine crystals with unique shapes and controlled size. Jpn J Appl Phys 2009;48:050206.
[8] Shrestha LK, Yamauchi Y, Hill JP, Miyazawa K, Ariga K. Fullerene crystals with bimodal pore architectures consisting of macropores and mesopores. J Am Chem Soc 2013;135:586–9.
[9] Nakanishi T, Schmitt W, Michinobu T, Kurth DG, Ariga K. Hierarchical supramolecular fullerene architectures with controlled dimensionality. Chem Comm 2005:5982–4.
[10] Nakanishi T, Ariga K, Michinobu T, Yoshida K, Takahashi H, Teranishi T, et al. Flower-shaped supramolecular assemblies: hierarchical organization of a fullerene bearing long aliphatic chains. Small 2007;3:2019–23.
[11] Zhang X, Takeuchi M. Controlled fabrication of fullerene C_{60} into microspheres of nanoplates through porphyrin-polymer-assisted self-assembly. Angew Chem Int Ed 2009;48:9646–51.
[12] Yao MG, Andersson BM, Stenmark P, Sundqvist B, Liu BB, Wagberg T. Synthesis and growth mechanism of differently shaped C_{60} nano/microcrystals produced by evaporation of various aromatic C_{60} solutions. Carbon 2009;47:1181–8.
[13] Shin HS, Yoon SM, Tang Q, Chon B, Joo T, Choi HC. Highly selective synthesis of C_{60} discs on graphite substrate by a vapor-solid process. Angew Chem Int Ed 2008;47:693–6.
[14] Akada M, Hirai T, Takeuchi J, Yamamoto T, Kumashiro R, Tanigaki K. Superconducting phase sequence in R_xC_{60} fullerides (R = Sm and Yb). Phys Rev B 2006;73:094509.
[15] Takeya H, Miyazawa K, Kato R, Wakahara T, Ozaki T, Okazaki H, et al. Superconducting fullerene nanowhiskers. Molecules 2012;17:4851–9.
[16] Yang F, Forrest SR. Organic solar cells using transparent SnO_2-F anodes. Adv Mater 2006;18:2018–22.
[17] Somani PR, Somani SP, Umeno M. Toward organic thick film solar cells: three dimensional bulk heterojunction organic thick film solar cell using fullerene single crystal nanorods. Appl Phys Lett 2007;91:173503.
[18] Ogawa K, Kato T, Ikegami A, Tsuji H, Aoki N, Ochiai Y, et al. Electrical properties of field-effect transistors based on C_{60} nanowhiskers. Appl Phys Lett 2006;88:112109.
[19] Kasai H, Nalwa HS, Oikawa H, Okada S, Matsuda H, Minami N, et al. A novel preparation method of organic microcrystals. Jpn J Appl Phys 1992;31:L1132.
[20] Nalwa HS, Kasai H, Okada S, Oikawa H, Matsuda H, Kakuta A, et al. Fabrication of organic nanocrystals for electronics and photonics. Adv Mater 1993;5:758–60.
[21] Kasai H, Okazaki S, Hanada T, Okada S, Oikawa H, Adschiri T, et al. Preparation of C_{60} microcrystals using high temperature and high pressure liquid crystallization method. Chem Lett 2000:1392–3.
[22] Korobov MV, Stukalin EB, Mirakyan AL, Neretin IS, Slovokhotov YL, Dzyabchenko AV, et al. New solid solvates of C_{60} and C_{70} fullerenes: The relationship between structures and lattice energies. Carbon 2003;41:2743–55.
[23] Heiney PA, Fischer JE, Mcghie AR, Romanow WS, Denenstein AM, Mccauley JP, et al. Orientational ordering transition in solid C_{60}. Phys Rev Lett 1991;67:2911–4.
[24] Minato J, Miyazawa K, Suga T. Morphology of C_{60} nanotubes fabricated by the liquid–liquid interfacial precipitation method. Sci Technol Adv Mater 2005;6:272–7.
[25] Rauwerdink K, Liu J-F, Kintigh J, Miller GP. Thermal, sonochemical, and mechanical behaviors of single crystal [60]fullerene nanotubes. Micros Res Tech 2007;70:513–21.
[26] Skokan EV, Arkhangelskii IV, Izotov DE, Chelovskaya NV, Nikulin MM, Velikodnyi YA. Stability of hexagonal modification of fullerite C_{60}. Carbon 2005;43:803–8.
[27] Sathish M, Miyazawa K, Hill JP, Ariga K. Solvent engineering for shape-shifter pure fullerene (C60). J Am Chem Soc 2009;131:6372–3.
[28] Masuhara A, Tan Z, Ikeshima M, Sato T, Kasai H, Oikawa H, et al. Cyclic transformation in shape and crystal structure of C_{60} microcrystals. Cryst Eng Comm 2012;14:7787–91.
[29] Peters D. Ultrasound in materials chemistry. J Mater Chem 1996;6:1605–18.
[30] Gedanken A. Using sonochemistry for the fabrication of nanomaterials. Ultrason Sonochem 2004;11:47–55.
[31] Mayers B, Xia YN. Formation of tellurium nanotubes through concentration depletion at the surfaces of seeds. Adv Mater 2002;14:279–82.
[32] Qu Y, Yu W, Liang S, Li S, Zhao J, Piao G. Structure and morphology characteristics of fullerene C_{60} nanotubes fabricated with n-methyl-2-pyrrolidone as a good solvent. J Nanomater 2011;3:706293. http://dx.doi.org/10.1155/2011/706293.
[33] Tan Z. Morphology-controlled fullerene microcrystals and their hybridization. Sendai, Japan: Tohoku University, PhD thesis; 2008.